Int J Cardiovasc Imaging (2013) 29:1351–1360
DOI 10.1007/s10554-013-0207-9

ORIGINAL PAPER

Computed tomography calcium score scan for attenuation correction of N-13 ammonia cardiac positron emission tomography: effect of respiratory phase and registration method

Habib Zaidi · Rene Nkoulou · Sarah Bond · Aylin Baskin · Thomas Schindler · Osman Ratib · Jerome Declerck

Received: 25 December 2012 / Accepted: 12 March 2013 / Published online: 17 March 2013

Abstract The use of coronary calcium scoring (CaScCT) for attenuation correction (AC) of ^{13}N-ammonia PET/CT studies (NH_3) is still being debated. We compare standard ACCT to CaScCT using various respiratory phases and co-registration methods for AC. Forty-one patients underwent a stress/rest NH_3. Standard ACCT scans and CaScCT acquired during inspiration (CaScCTinsp, 26 patients) or expiration (CaScCTexp, 15 patients) were used to correct PET data for photon attenuation. Resulting images were compared using Pearson's correlation and Bland–Altman (BA) limits of agreement (LA) on segmental relative and absolute coronary blood flow (CBF) using both manual and automatic co-registration methods (rigid-body and deformable). For relative perfusion, CaScCTexp correlates better than CaScCTinsp with ACCT when using manual co-registration ($r = 0.870$; $P < 0.001$ and $r = 0.732$; $P < 0.001$, respectively). Automatic co-registration provides the best correlation between CaScCTexp and ACCT for relative perfusion ($r = 0.956$; $P < 0.001$). Both CaScCTinsp and CaScCTexp yielded excellent correlations with ACCT for CBF when using manual co-registration ($r = 0.918$; $P < 0.001$; BA mean bias 0.05 ml/min/g; LA: −0.42 to +0.3 ml/min/g and $r = 0.97$; $P < 0.001$; BA mean bias 0.1 ml/min/g; LA: −0.65 to +0.5 ml/min/g, respectively). The use of CaScCTexp and deformable co-registration is best suited for AC to quantify relative perfusion and CBF enabling substantial radiation dose reduction.

Keywords PET/CT · Cardiac imaging · Attenuation correction · Calcium scoring · Quantification

H. Zaidi (✉) · R. Nkoulou · A. Baskin · O. Ratib
Division of Nuclear Medicine and Molecular Imaging, Geneva University Hospital, 1211 Geneva 4, Switzerland
e-mail: habib.zaidi@hcuge.ch

H. Zaidi
Geneva Neuroscience Center, Geneva University, 1205 Geneva, Switzerland

H. Zaidi
Department of Nuclear Medicine and Molecular Imaging, University of Groningen, University Medical Center Groningen, 9700 RB Groningen, The Netherlands

S. Bond · J. Declerck
Siemens Healthcare, Molecular Imaging, 23-38 Hythe Bridge Street, Oxford OX1 2EP, UK

T. Schindler
Cardiovascular Center, Nuclear Cardiology, Geneva University, 1211 Geneva, Switzerland

Introduction

Myocardial perfusion imaging (MPI) using PET/CT is a non-invasive procedure allowing the functional assessment of coronary artery disease (CAD) with a reported higher diagnostic accuracy compared to MPI SPECT, particularly in the obese population and in patients undergoing pharmacologic stress [1]. Other definite advantages of PET/CT are higher and temporal spatial resolution, higher sensitivity, simultaneous whole heart acquisition and more accurate depth-dependent activity recovery owing to robust CT-based attenuation correction [2]. These, along with suitable tracer kinetics have enabled reproducible quantification of absolute coronary blood flow.

Absolute coronary blood flow quantification and coronary flow reserve have proved to provide added prognostic

value in a wide range of cardiovascular diseases [3]. However, reimbursement issues, tracers and PET/CT systems availability have until now limited the spread of MPI PET/CT. Strengthening the gathered evidence from MPI PET, including a better standardization and comparison of current acquisition and processing protocols will undoubtedly fuel the growing appraisal of this technique [4].

Attenuation correction (AC) is usually performed using several low dose CT scans to limit the misalignment potentiated by the long time interval between each PET acquisition [5]. This is followed by alignment with PET images prior to attenuation correction of PET data [6–11]. More refined strategies were proposed to correct for photon attenuation in cardiac PET/CT imaging including phased AC [12], respiration-averaged CT [13, 14], aligning a single CT with each frame of a gated PET study [15, 16], contrast-enhanced CT with appropriate correction for contrast media [17], and interpolated average CT [18], but these have so far failed to gain wide clinical acceptance.

Coronary artery calcium scoring CT (CaScCT), providing an estimate of global atherosclerotic burden and risk stratification beyond traditional coronary risk factors, is frequently assessed during MPI procedures. The relevance of formal calcium scores in terms of patient management is a controversial issue which falls outside the scope of this work [19, 20]. In an effort to reduce as much as possible the radiation dose delivered to the patient, few preliminary reports have evaluated the feasibility of using CaScCT for AC of NH_3 MPI studies [21, 22]. Alternatively, the use of the traditional AC scan for depicting calcium burden has been proposed but reported to underestimate it in case of high calcium burden [23]. When using CaScCT for AC, special attention has to be paid to proper alignment of PET and CaScCT datasets. This is particularly the case for NH_3-based MPI, a radiotracer with a half life of 10 min with mandatory long time interval between stress and rest acquisition potentiating misalignment. In this regard, selecting an optimal co-registration method is the key to providing reproducible results without excessive post-processing. Another concern when using CaScCT for AC is the selection of the respiratory phase, with inspiration CaScCT being more suitable for the detection ancillary pulmonary findings but acquired in a chest position more distant to the average chest position corresponding to prolonged PET acquisitions.

The aim of the present study is therefore to introduce a comprehensive framework for using coronary calcium scoring images for AC of myocardial perfusion PET/CT images combined with various image registration methods and respiratory phases during acquisition aiming at devising an optimized acquisition and processing protocol with reduced absorbed dose to the patient.

Materials and methods

Study population

Forty-one consecutive patients (26 male; 15 female) with intermediate pre-test probability of CAD and referred for a rest–stress NH_3-PET perfusion study were enrolled in this study protocol. Their mean age was 49 ± 14 years (range 29–77 years). Baseline characteristics of the study participants are detailed in Table 1. Approval was obtained from the institutional ethics committee and all patients provided written informed consent.

Data acquisition protocol

Data acquisition was performed using a Biograph 64 True Point PET/CT scanner (Siemens Healthcare, Erlangen, Germany) offering advanced cardiovascular imaging capabilities including volumetric CT to visualize the anatomy of the heart's blood vessels. The PET subsystem consists of 24,336 lutetium oxyorthosilicate (LSO) crystals ($4 \times 4 \times 25$ mm^3) arranged in 39 rings and operating in a fully three-dimensional mode with an axial field-of-view of 162 mm. The CT subsystem consists of a 40-rows ceramic detector with 1'344 channels per row using adaptive collimation and the z-sharp technique to acquire 64 slices per rotation.

After a localisation scout scan, a standard low-dose transmission CT scan with shallow breathing was performed for attenuation correction (CTAC) before rest and stress (120 kVp, 74 effective mAs, 24 × 1.2 collimation, 0.45:1 pitch, 1 s rotation time). In addition, an Electrocardiographic (ECG)-gated Calcium score CT (CaScCT) was acquired during breath-hold (inspiration or expiration) using the following scan parameters: tube current 120 kVp, effective tube voltage 190 mAs, 24 × 1.2 collimation, 0.2:1 pitch and 0.33 s per gantry rotation. CaScCT was acquired at inspiration for the first group (26 patients) and at expiration for the second group (15 patients) of patients. The level of calcium present in this population was relatively low.

Table 1 Baseline characteristics of the study population

Characteristic	
Number	41
Age	49 ± 14.9
Gender	Male 70 %, female 30 %
BMI[a]	33 ± 8
Calcium score (Agtaston score)	125 ± 376
LVEF (%)[b]	52 ± 9

[a] *BMI* body mass index in kg/m^2

[b] *LVEF* left ventricular ejection fraction

Dynamic PET data acquisition was initiated along with injection of radiotracer bolus (500 MBq of ^{13}N-ammonia) in list-mode format during 6 min followed immediately by ECG-gated PET data acquisition for 18 min at rest and repeated under stress following a second CTAC scan, 3 min after slow Dipyridamole infusion (140 μg/kg/min during 4 min). The data acquisition protocol is shown in Fig. 1. Calcium scoring and CT angiography are routinely used in our institution.

Data processing

The standard low-dose transmission CT scan was reconstructed using a B10s kernel filter and 2.0 mm slice increment. The CaScCT was reconstructed with an extended FOV (700 mm) in contrast to the standard reconstruction used for coronary calcium burden evaluation (200 mm FOV).

For the PET image dataset, dynamic series encompassing the first 6 min (12 × 10 s, 3 × 20 s, 6 × 30 s frames) were used for absolute flow quantification whereas ECG-gated series (8 phases) encompassing the last 12 min of acquisitions were used for relative perfusion quantification. Non attenuated corrected (NAC) images were reconstructed using statistical iterative reconstruction (OSEM) (168 × 168; 4 iterations, 8 subsets) followed by Gaussian smoothing (FWHM 5 mm).

The attenuated corrected (AC) PET series generated after co-registering NAC series with low-dose CT (ACCT) were compared to those obtained using CaScCT for attenuation correction instead of the low-dose CT. To determine the optimal registration procedure, various registration methods were tested, namely manual registration, rigid-body automatic registration using the AutoCardiac software (Siemens Healthcare, Hoffman Estates, IL, USA) and using mutual information based deformable registration algorithm [10].

Assessment strategy

Relative perfusion quantification

Static perfusion PET series were evaluated using the 4D-M SPECT software (Invia, AnnArbor, MI, USA). After reorientation into short axis, vertical and horizontal long axis views, perfusion polar map were generated and displayed as per-segment values in a standardized 17-segment bull-eye plot as proposed by the American Heart Association (AHA) [24]. The summed stress score (SSS) and summed difference score (SDS) defined as the difference between SSS and summed difference score were reported when using CTAC and CaScCT for attenuation correction of PET data.

Absolute coronary blood flow

Dynamic PET series were evaluated using the *syngo* MBF software [25] (Siemens Healthcare, Hoffman Estates, IL, USA). Regions of interest in the right ventricle, left ventricle and encompassing the left ventricular myocardium were automatically generated. A 2-tissue compartment model described by Hutchins et al. [26] was used to derive absolute coronary flow values in ml/min/g for the three main coronary territories following the segmentation proposed by the AHA [24]. Coronary flow reserve (CFR) was calculated as the ratio of stress to rest absolute blood flow.

Statistical analysis

Values were expressed as mean ± SD or median with interquartile range (IQR). Means were compared using a paired t test. Coronary vessel flow values and myocardial segmental uptake values obtained using CaScCT and different methods were compared to those obtained using low-dose CT and manual registration taken as reference

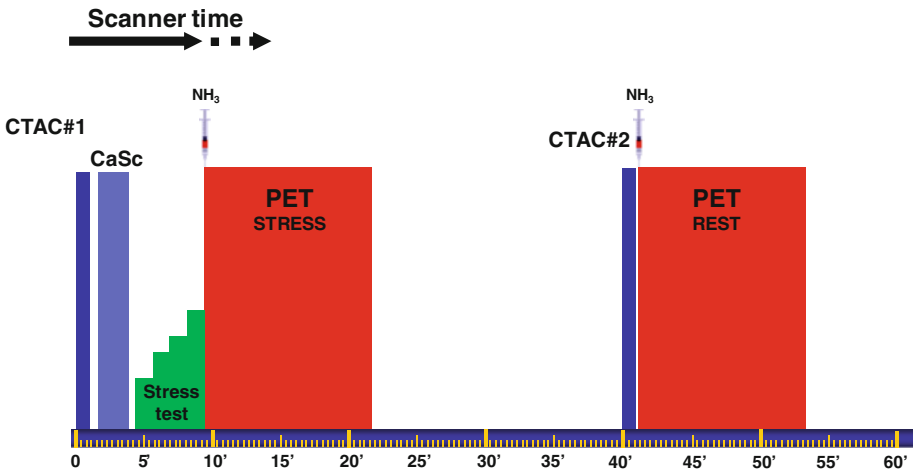

Fig. 1 Workflow of the ^{13}N-ammonia PET/CT data acquisition protocol

since it is the most widely used approach in the clinic. The Pearson's correlation was expressed by the correlation coefficient and slope of the regression line. The correlation coefficients were also compared using similar statistical tests. Systematic biases were illustrated by Bland and Altman limits of agreement. *P* values of less than 0.05 were considered statistically significant.

Results

All clinical PET studies were corrected for attenuation using the corresponding low-dose CT (ACCT1 or ACCT2) and CaScCT. The mean dose length product for ACCT and CaScCT scans were 94 and 141 mGy.cm, resulting in effective doses of 1.5 and 2.3 mSv, respectively. A representative example of the registration of the CaScCT to the NAC PET images is presented in Fig. 2.

Relative perfusion quantification

The visual assessment of perfusion scans revealed a normal finding in 27 patients, reversible perfusion defects in 9 patients and fixed perfusion defect pattern in 5 patients. The difference between SSS using CTAC and CaSC with manual, automatic rigid-body or deformable co-registration was within 1 point in 61, 97.6 and 90.2 % of the patients, respectively. Figures 3, 4 and 5 display the correlation plots between CaScCT acquired with different breathing patterns and aligned using various co-registration techniques and ACCT aligned using manual co-registration. Overall, segmental perfusion values using CaScCT correlated well with those obtained using ACCT after manual registration ($r = 0.787$; $P < 0.001$; Bland and Altman mean bias −0.3 limits of agreement: −6.3 to 5.6, SEE = 0.15) (Fig. 3a). However, significantly higher correlation was observed when attenuation correction is performed using CaScCT acquired at expiration ($r = 0.870$; $P < 0.001$; Bland and Altman mean bias −0.9 limits of agreement: −4.9 to 3.0; SEE = 0.21) (Fig. 3c) compared to CaScCT acquired at inspiration ($r = 0.732$; $P < 0.001$; Bland and Altman mean bias 0.0 limits of agreement: −4.9 to 5.0; SEE = 0.21) (Fig. 3b). The difference between the two correlations was also statistically significant ($P < 0.05$). In patients with CaScCT acquired at inspiration, the use of automatic rigid-body co-registration yielded a correlation of $r = 0.881$ ($P < 0.001$; Bland and Altman mean bias 0.3 limits of agreement: −4.6 to 5.3; SEE = 0.15) (Fig. 4b) whereas the use of automatic deformable co-registration deteriorated the correlation ($r = 0.576$; $P < 0.001$; Bland and Altman mean bias 1.6 limits of agreement: −8.3 to 11.6; SEE = 0.31) (Fig. 5b). In patients with CaScCT acquired at expiration, equivalent correlation was observed between manual and automatic rigid-body co-registration ($r = 0.870$; $P < 0.001$; Bland and Altman mean bias −0.9 limits of agreement: −4.9

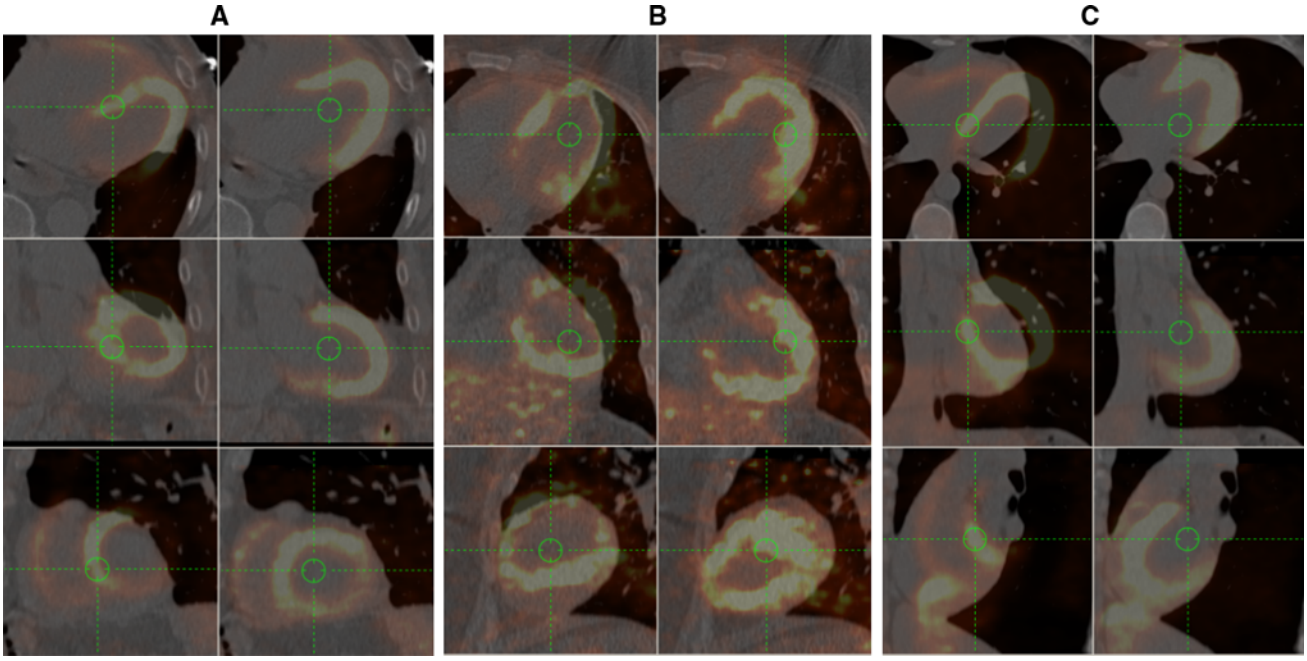

Fig. 2 Representative example of the co-registration procedure of the CaScCT acquired in end inspiration to the uncorrected PET images. The *three rows* **a**, **b** and **c** represent the transaxial, coronal and sagittal views of registration of the calcium score CT to PET images. *Columns 1*, *3* and *5* are before co-registration while *columns 2*, *4*, *6* are after co-registration

to 3.0; SEE = 0.21) (Fig. 4c) whereas a much higher correlation was achieved using deformable co-registration (r = 0.956; $P < 0.001$; Bland and Altman mean bias −0.3 limits of agreement: −2.8 to 2.1; SEE = 0.13) (Fig. 5c). The difference between rigid-body and deformable co-registrations was also statistically significant ($P < 0.05$). The Bland and Altman plots shown in Fig. 6 indicate that the bias is significantly reduced when using CaScCTexp.

The correlation of 17-segment perfusion values comparing CaScCTinsp alignments to the manual ACCT alignment are shown in Fig. 7. It can be seen that the differences occur in outer segments and these differences are likely averaged out in the flow comparison as only 3-segments are recorded. Differences are also likely due to the nature of the scan. ACCT are taken at shallow free breathing and therefore are most likely to be at expiration, whereas the CaScCTinsp are taken at breath hold inspiration.

Tables 2 and 3 summarize the correlations and Bland and Altman limits of agreement obtained for global and regional relative perfusion both at inspiration and expiration, emphasizing a closer correlation and narrower limit of agreement obtained using the expiration CaScCT scan. Improved correlation is observed when using expiration breathing phase. Minimal bias (in percent of regional uptake values) is observed when using either breathing phase or co-registration method.

Absolute perfusion quantification

The global CBF at rest and stress using ACCT scan was 0.90 ± 0.28 and 2.30 ± 0.84 ml/min/g, respectively. The global CFR was 2.84 ± 1.45 among the 41 study participants. A CFR below 2 was observed in 13 patients.

The global CBF obtained using CaScCT scan acquired at inspiration correlated well with values obtained using ACCT after manual co-registration (r = 0.92; $P < 0.001$; Bland and Altman mean bias 0.1 ml/min/g limits of agreement: −0.65 to +0.5 ml/min/g; SEE = 0.03), automatic rigid-body co-registration (r = 0.90; $P < 0.001$; Bland and Altman mean bias 0.05 ml/min/g limits of agreement: −0.60 to +0.55 ml/min/g; SEE = 0.03) and deformable co-registration (r = 0.918; $P < 0.001$; Bland and Altman mean bias 0.05 ml/min/g limits of agreement: −0.55 to +0.55 ml/min/g; SEE = 0.03). Similarly, CaScCT scans acquired at expiration also yielded excellent correlations when using manual co-registration (r = 0.97; $P < 0.001$; Bland and Altman mean bias 0.05 ml/min/g limits of agreement: −0.42 to +0.3 ml/min/g; SEE = 0.03), automatic rigid-body co-registration (r = 0.96; $P < 0.001$; Bland and Altman mean bias 0.02 ml/min/g limits of agreement: −0.55 to +0.5 ml/min/g; SEE = 0.04) or deformable co-registration (r = 0.966; $P < 0.001$; Bland and Altman mean bias 0.02 ml/min/g limits of agreement: −0.40 to +0.5 ml/min/g; SEE = 0.04).

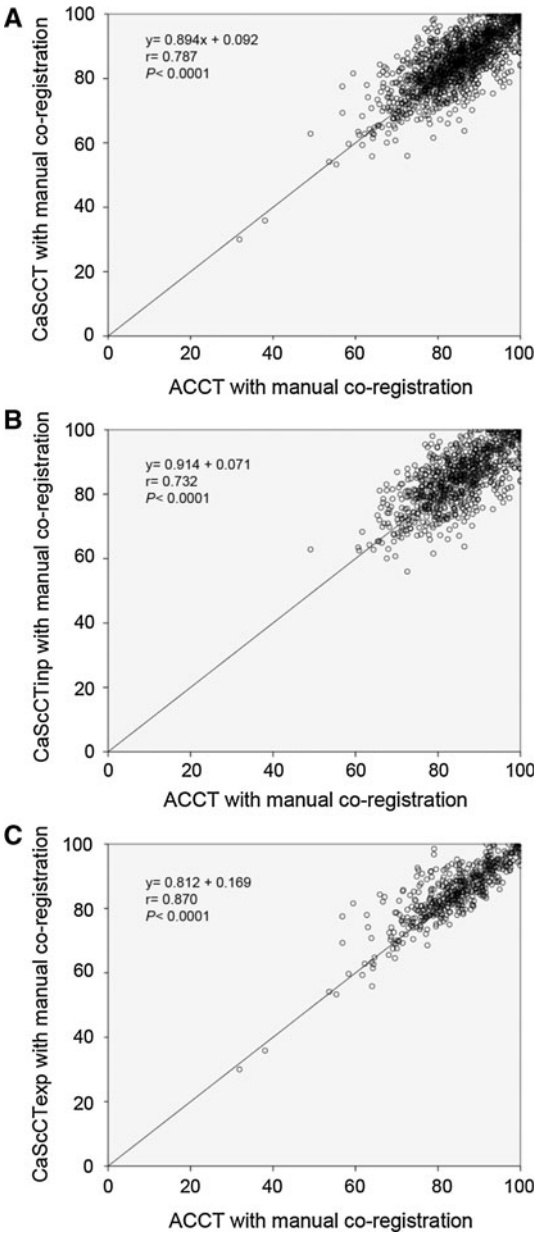

Fig. 3 Correlation between relative segmental uptake values when using CTAC and CaScCT using manual co-registration for all patients (**a**), for patients acquired at inspiration (**b**) and for patients acquired at expiration (**c**). CaScCT = PET corrected for attenuation with coronary calcium score CT scan. CaScCTinsp = calcium score CT scan acquired at inspiration. CaScCTexp = calcium score CT scan acquired at expiration. ACCT = PET corrected for attenuation with standard CT scan

Tables 4 and 5 summarize the correlations and Bland and Altman limits of agreement obtained for global and regional CFR both at inspiration and expiration, emphasizing a closer correlation and narrower limit of agreement obtained using the expiration CaScCT scan. Better correlation is perceived when using expiration breathing phase. Minimal bias in flow values is observed when using either breathing phase or co-registration method.

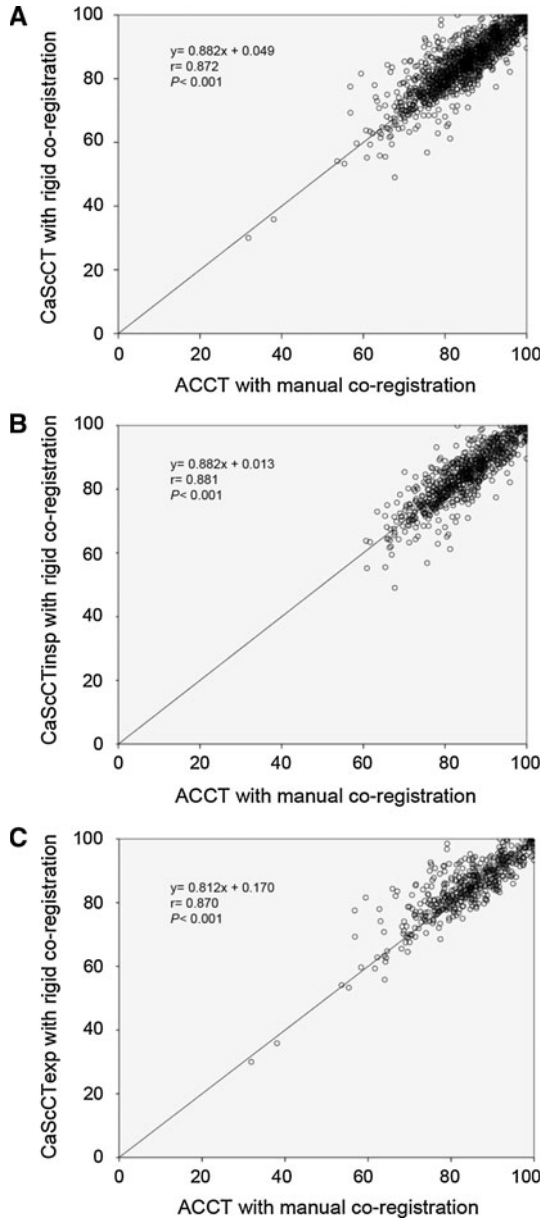

Fig. 4 Correlation between relative segmental uptake values when using CTAC and CaScCT using automatic rigid-body co-registration for all patients (**a**) for patients acquired at inspiration (**b**) and for patients acquired at expiration (**c**). CaScCT = PET corrected for attenuation with coronary calcium score CT scan. CaScCTinsp = calcium score CT scan acquired at inspiration. CaScCTexp = calcium score CT scan acquired at expiration. ACCT = PET corrected for attenuation with standard CT scan

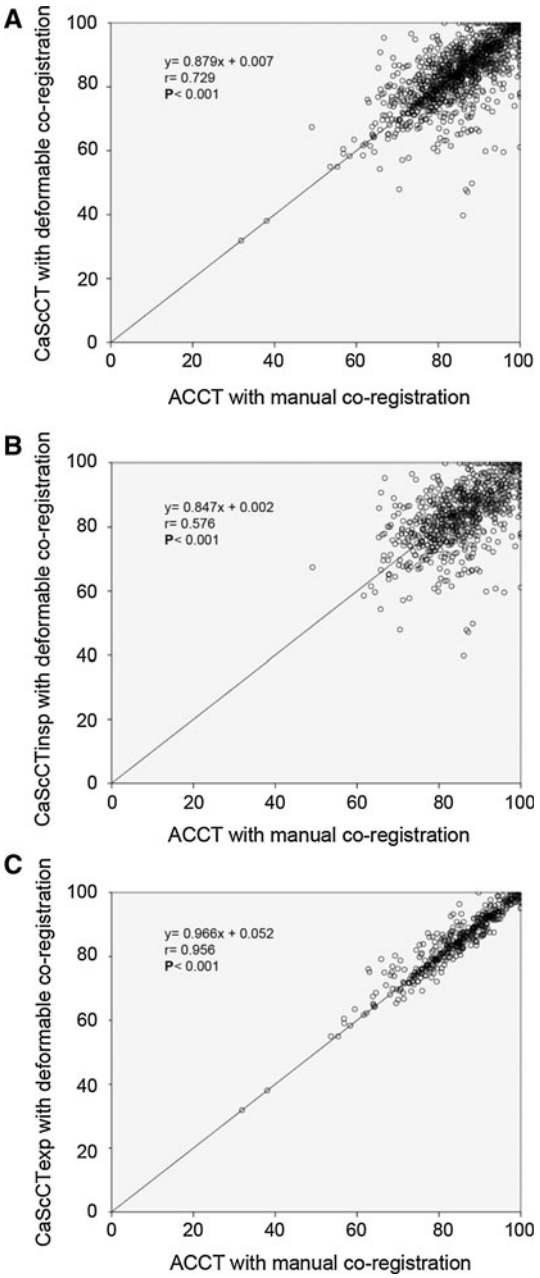

Fig. 5 Correlation between relative segmental uptake values when using CTAC and CaScCT using deformable co-registration for all patients (**a**) for patients acquired at inspiration (**b**) and for patients acquired at expiration (**c**). CaScCT = PET corrected for attenuation with coronary calcium score CT scan. CaScCTinsp = calcium score CT scan acquired at inspiration. CaScCTexp = calcium score CT scan acquired at expiration. ACCT = PET corrected for attenuation with standard CT scan

Discussion

Hybrid PET/CT imaging scanners with CT subsystems having large axial field-of-view coverage, thus allowing high temporal resolution are particularly suited for diagnosis and prognosis of coronary artery disease. However, the radiation burden associated with typical high dose cardiovascular imaging protocols remains a sensitive issue that needs to be addressed through dedicated dose-saving protocols [27]. Calcium scoring is routinely used in the clinic and is considered as the marker of choice for the prediction of the extension of heart disease in medium risk CAD patients. Feasibility studies reported on the potential use of calcium score for attenuation correction of cardiac

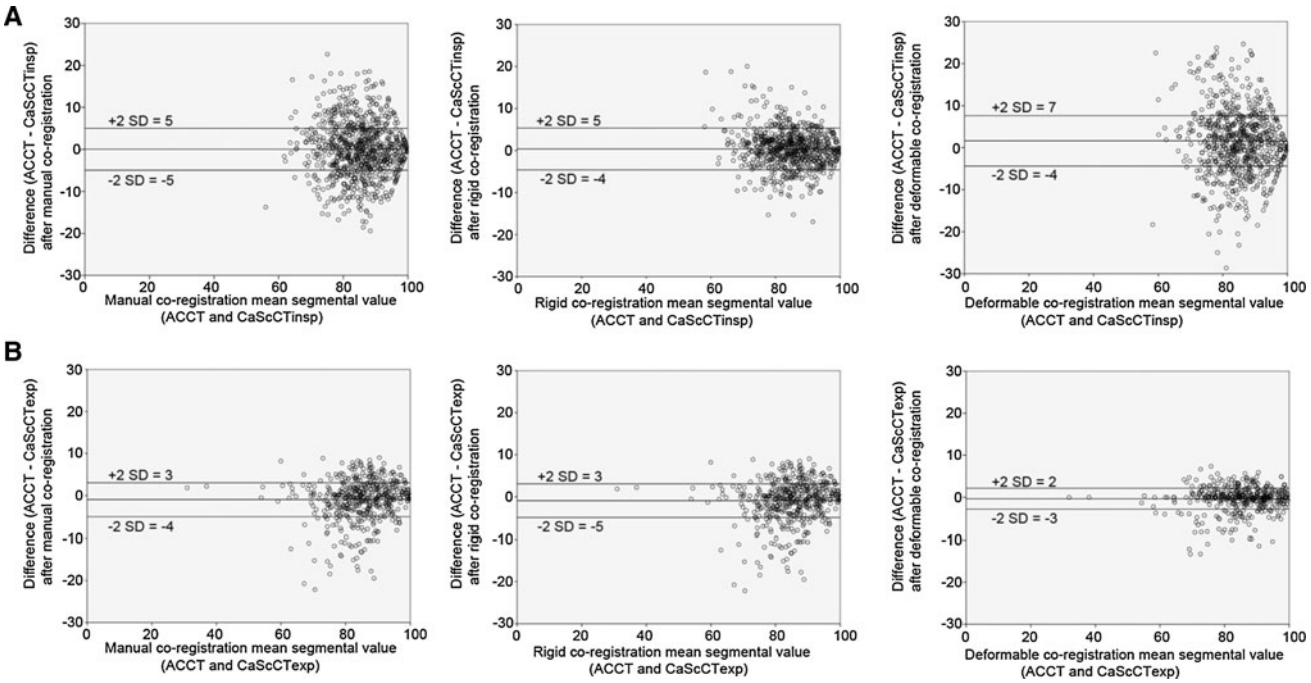

Fig. 6 Bland–Altmann plots representation for comparison between **a** inspiration and **b** expiration when using manual (*left panel*), automatic rigid-body (*middle panel*) and automatic deformable (*right panel*) co-registration. CaScCT = PET corrected for attenuation with coronary calcium score CT scan. CaScCTinsp = calcium score CT scan acquired at inspiration. CaScCTexp = calcium score CT scan acquired at expiration. ACCT = PET corrected for attenuation with standard CT scan

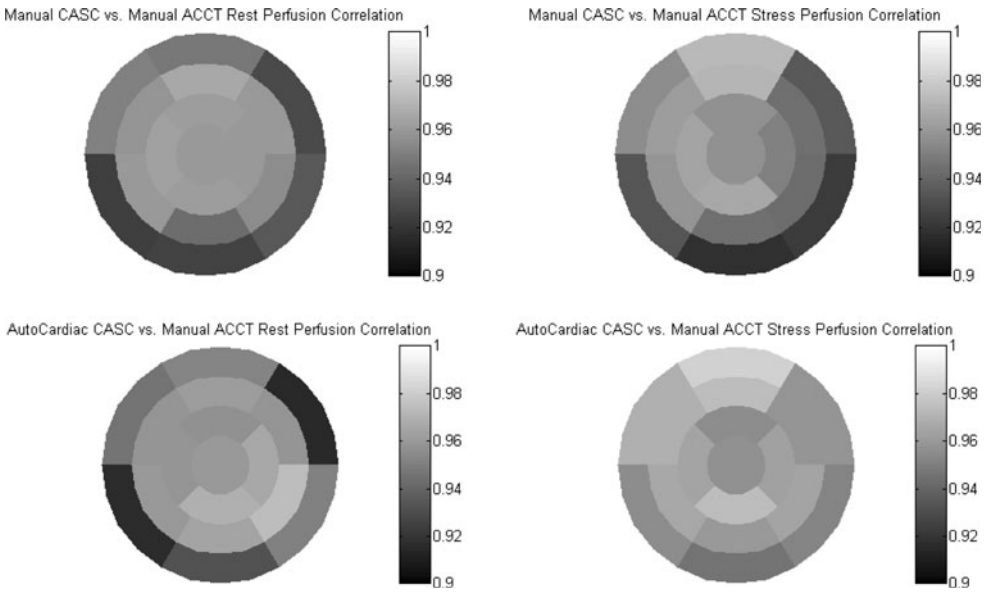

Fig. 7 *Top left* correlation of rest perfusion of manual alignment applied to CaScCT compared to the manual alignment of the ACCT. *Top right* correlation of stress perfusion of manual alignment applied to CaScCT compared to the manual alignment of the ACCT. *Bottom left* correlation of rest perfusion of rigid-body alignment applied to CaScCT compared to the manual alignment of the ACCT. *Bottom right* correlation of stress perfusion of rigid-body alignment applied to CaScCT compared to the manual alignment of the ACCT

rest/stress NH_3 perfusion and FDG viability PET/CT studies [21, 22]. Therefore, the availability of the calcium score exam could be exploited to reduce the dose delivered to the patient by eliminating the need of acquiring two additional (3 for some research protocols involving a 3rd acquisition, e.g., cold pressure test—CPT) low-dose CT scans for attenuation correction of PET data. For patient populations that do not require a calcium score scan, the protocol could be modified by using only one instead of 2 or 3 low-dose CT scans for attenuation correction.

Our results show that fairly large image transformations are required to align CaScCT to NAC PET images for the purpose of attenuation correction. These large transformations can be performed manually through rigid transformation, or automatically through either rigid-body or deformable registration. The performance of automatic registration algorithms was

Table 2 Correlation coefficients between global and regional relative perfusion obtained using CaScCT-based attenuation correction and low-dose CT-based attenuation correction with manual co-registration

Correlation	CASC manual		CASC auto		CASC deformable	
	Inspiration	Expiration	Inspiration	Expiration	Inspiration	Expiration
Global	0.73	0.87	0.88	0.87	0.57	0.95
LAD	0.77	0.93	0.88	0.93	0.54	0.95
CX	0.75	0.84	0.87	0.84	0.56	0.95
RCA	0.69	0.78	0.93	0.78	0.64	0.96

LAD left anterior descending artery territory, *CX* circumflex artery territory, *RCA* right coronary artery territory

CaScCT: perfusion dataset corrected for attenuation using calcium CT scan; *manual:* manual co-registration; *rigid:* rigid co-registration; *deformable:* deformable co-registration

Table 3 Mean global and regional absolute relative perfusion bias obtained using CaScCT-based attenuation correction compared to low-dose CT-based attenuation correction with manual co-registration according to the breath-hold phase

Bias (in %)	CaScCT manual		CaScCT auto		CaScCT deformable	
	Inspiration	Expiration	Inspiration	Expiration	Inspiration	Expiration
Global	0.1 (2.5)	0.0 (1.8)	0.0 (2.3)	0.1 (2.0)	1 (2.8)	0 (1.3)
LAD	−0.9 (5.4)	0.1 (3.7)	1.7 (3.9)	0.1 (3.7)	1.9 (6.9)	0.2 (3.1)
CX	1.0 (6.0)	0.4 (4.2)	1.9 (4.1)	0.4 (4.2)	0.6 (6.5)	1.0 (2.5)
RCA	0.3 (7.4)	3.0 (6.1)	0.5 (3.6)	3.0 (6.1)	0.5 (7.4)	0.5 (2.8)

LAD left anterior descending artery territory, *CX* circumflex artery territory, *RCA* right coronary artery territory

CaScCT: perfusion dataset corrected for attenuation using calcium CT scan; *manual:* manual co-registration; *rigid:* rigid co-registration; *deformable:* deformable co-registration

Table 4 Correlation coefficients between global and regional absolute flow obtained using CaScCT-based attenuation correction and low-dose CT-based attenuation correction with manual co-registration

Correlation coefficient	CaScCT manual		CaScCT rigid		CaScCT deformable	
	Inspiration	Expiration	Inspiration	Expiration	Inspiration	Expiration
Global	0.90	0.99	0.96	0.98	0.95	0.97
LAD	0.88	0.99	0.93	0.99	0.94	0.91
CX	0.93	0.99	0.97	0.99	0.95	0.97
RCA	0.91	0.98	0.98	0.99	0.91	0.98

LAD left anterior descending artery territory, *CX* circumflex artery territory, *RCA* right coronary artery territory

CaScCT: flow dataset corrected for attenuation using calcium CT scan; *manual:* manual co-registration; *rigid:* rigid co-registration; *deformable:* deformable co-registration

Table 5 Mean global and regional absolute flow bias obtained using CaScCT-based attenuation correction compared to low-dose CT-based attenuation correction with manual co-registration according to the breath-hold phase

Bias in ml/min/g (SD)	CaScCT manual		CaScCT rigid		CaScCT deformable	
	Inspiration	Expiration	Inspiration	Expiration	Inspiration	Expiration
Global	0.08 (0.61)	0.10 (0.18)	−0.02 (0.41)	0.06 (0.17)	−0.02 (0.39)	0.12 (0.47)
LAD	0.06 (0.66)	0.10 (0.23)	−0.41 (0.48)	0.07 (0.19)	−0.11 (0.50)	0.20 (0.77)
CX	0.04 (0.52)	0.09 (0.17)	−0.22 (0.35)	−0.01 (0.14)	0.17 (0.46)	−0.10 (0.36)
RCA	0.18 (0.69)	0.17 (0.26)	−0.00 (0.37)	0.14 (0.19)	0.17 (0.46)	0.18 (0.28)

LAD left anterior descending artery territory, *CX* circumflex artery territory, *RCA* right coronary artery territory

CaScCT: flow dataset corrected for attenuation using calcium CT scan; *manual:* manual co-registration; *rigid:* rigid co-registration; *deformable:* deformable co-registration

assessed through comparison to manual alignment which gave well correlated results in terms of relative perfusion and absolute flow values. It must be noted that both dedicated cardiac data processing applications used in this work (4DM SPECT and syngoMBF) employ automatic segmentation techniques, which if performing differently using the datasets being compared, could lead to small differences in the final perfusion and flow values.

Such large misalignments of the CaScCT images indicate a need for reproducible and observer independent software-based registration. Aligning PET and CT datasets for the purpose of AC can be time consuming and the obtained results are often inconsistent. An automatic method can provide a good first estimate of the registration, and while it would always be required to check for any remaining misalignments or artefacts, such an automatic algorithm can considerably reduce the processing time.

The proposed method involving the use of the CaScCTexp scan outperforms the one using CaScCTinsp and achieves its best performance when combined with the deformable co-registration procedure in terms of correlation with the manually aligned ACCT scan. Moreover, the improvements brought by the deformable co-registration procedure are visually obvious and the technique has the additional advantage of being user-independent and reproducible. A very high correlation was obtained between the deformably registered CaScCT and manually aligned ACCT. However, in the absence of gold standard for comparison, it is unclear whether the results of flow and perfusion are more accurate using this technique compared to other algorithms assessed in this work. Further experiments across multiple datasets are required to proof consistency of the deformable alignment procedure. While the results were obtained using a relatively small patient population, they look promising to warrant further evaluation using a larger study population. Since statistical significance does not always lead to clinical significance, further research is guaranteed to assess the effect of the proposed methodology on the clinical outcome of patients.

An alternative attenuation correction method involving the use of only the CaScCT eliminates the need for 2 low-dose CT scans required for ACCT and therefore reduces the effective dose to the patient by about 3 mSv. It should be noted that the radiation dose delivered to an adult from N-13 ammonia is $\sim$2 mSv total effective dose following injection of 1 GBq (2 $\times$ 500 MBq) [28].

Conclusions

We have demonstrated that the CaScCT scan can be used for attenuation correction of cardiac rest/stress PET data; however, large translations need to be performed prior to image reconstruction. Automatic methods are well suited to perform or aid the registration procedure, as required. The flow and perfusion results corrected for attenuation using the CaScCTinsp scan are consistent with those reported by Ghafarian et al. [21]. It was also observed that noticeable improvement could be obtained using a CaScCTexp for attenuation correction of cardiac perfusion PET studies to quantify relative perfusion and CBF, thus allowing the elimination of 2 ACCT scans and, as such, substantial reduction of patient dose.

Acknowledgments This work was supported by the Swiss National Science Foundation under grant SNSF 31003A-135576 and Geneva University Hospital under grant PRD-11-II-1.

Conflict of interest S.B. and J.D. are employees of Siemens Healthcare. The authors declare that they have no conflict of interest.

References

1. Di Carli M, Lipton M (eds) (2007) Cardiac PET and PET/CT imaging. Springer, New York
2. Zaidi H, Hasegawa BH (2003) Determination of the attenuation map in emission tomography. J Nucl Med 44:291–315
3. Herzog BA, Husmann L, Valenta I, Gaemperli O, Siegrist PT, Tay FM et al (2009) Long-term prognostic value of 13N-ammonia myocardial perfusion positron emission tomography added value of coronary flow reserve. J Am Coll Cardiol 54:150–156
4. El Fakhri G, Kardan A, Sitek A, Dorbala S, Abi-Hatem N, Lahoud Y et al (2009) Reproducibility and accuracy of quantitative myocardial blood flow assessment with (82)Rb PET: comparison with (13)N-ammonia PET. J Nucl Med 50:1062–1071
5. McQuaid S, Hutton B (2008) Sources of attenuation-correction artefacts in cardiac PET/CT and SPECT/CT. Eur J Nuc Med Mol Imaging 35:1117–1123
6. Loghin C, Sdringola S, Gould KL (2004) Common artifacts in PET myocardial perfusion images due to attenuation-emission misregistration: clinical significance, causes, and solutions. J Nucl Med 45:1029–1039
7. Koepfli P, Hany TF, Wyss CA, Namdar M, Burger C, Konstantinidis AV et al (2004) CT attenuation correction for myocardial perfusion quantification using a PET/CT hybrid scanner. J Nucl Med 45:537–542
8. Martinez-Möller A, Souvatzoglou M, Navab N, Schwaiger M, Nekolla SG (2007) Artifacts from misaligned CT in cardiac perfusion PET/CT studies: frequency, effects, and potential solutions. J Nucl Med 48:188–193
9. Lautamaki R, Brown T, Merrill J, Bengel F (2008) CT-based attenuation correction in 82Rb-myocardial perfusion PET/CT: incidence of misalignment and effect on regional tracer distribution. Eur J Nucl Med Mol Imaging 35:305–310
10. Bond S, Kadir T, Hamill J, Casey M, Platsch G, Burckhardt D, et al (2008) Automatic registration of cardiac PET/CT for attenuation correction. In: IEEE nuclear science symposium and medical imaging conference, Dresden, Germany, 19–25 Oct 2008, pp 5512–5517
11. Gould KL, Pan T, Loghin C, Johnson NP, Guha A, Sdringola S (2007) Frequent diagnostic errors in cardiac PET/CT due to misregistration of CT attenuation and emission PET images: a definitive analysis of causes, consequences, and corrections. J Nucl Med 48:1112–1121

12. Nagel CCA, Bosmans G, Dekker ALAJ, Ollers MC, De Ruysscher DKM, Lambin P et al (2006) Phased attenuation correction in respiration correlated computed tomography/positron emitted tomography. Med Phys 33:1840–1847
13. Pan T, Mawlawi O, Luo D, Liu HH, Chi PM, Mar MV et al (2006) Attenuation correction of PET cardiac data with low-dose average CT in PET/CT. Med Phys 33:3931–3938
14. Cook RAH, Carnes G, Lee T-Y, Wells RG (2007) Respiration-averaged CT for attenuation correction in canine cardiac PET/CT. J Nucl Med 48:811–818
15. McQuaid SJ, Lambrou T, Hutton BF (2011) A novel method for incorporating respiratory-matched attenuation correction in the motion correction of cardiac PET-CT studies. Phys Med Biol 56:2903–2915
16. Gould KL, Pan T, Loghin C, Johnson NP, Sdringola S (2008) Reducing radiation dose in rest-stress cardiac PET/CT by single poststress cine CT for attenuation correction: quantitative validation. J Nucl Med 49:738–745
17. Buther F, Stegger L, Dawood M, Range F, Schafers M, Fischbach R et al (2007) Effective methods to correct contrast agent-induced errors in PET quantification in cardiac PET/CT. J Nucl Med 48:1060–1068
18. Wu T-H, Zhang G, Wang S-J, Chen C-H, Yang B-H, Wu N-Y et al (2010) Low-dose interpolated average CT for attenuation correction in cardiac PET/CT. Nucl Instrum Methods Phys Res A 619:361–364
19. Greenland P, Bonow RO, Brundage BH, Budoff MJ, Eisenberg MJ, Grundy SM et al (2007) ACCF/AHA 2007 clinical expert consensus document on coronary artery calcium scoring by computed tomography in global cardiovascular risk assessment and in evaluation of patients with chest pain: a report of the American College of Cardiology Foundation Clinical Expert Consensus Task Force (ACCF/AHA Writing Committee to Update the 2000 Expert Consensus Document on Electron Beam Computed Tomography) developed in collaboration with the Society of Atherosclerosis Imaging and Prevention and the Society of Cardiovascular Computed Tomography. J Am Coll Cardiol 49:378–402
20. Wexler L (2008) What is the value of measuring coronary artery calcification? Radiology 246:1–2
21. Ghafarian P, Aghamiri SM, Ay MR, Fallahi B, Rahmim A, Schindler TH et al (2010) Coronary calcium score scan-based attenuation correction in cardiovascular PET imaging. Nucl Med Commun 31:780–787
22. Burkhard N, Herzog BA, Husmann L, Pazhenkottil AP, Burger IA, Buechel RR et al (2010) Coronary calcium score scans for attenuation correction of quantitative PET/CT (13)N-ammonia myocardial perfusion imaging. Eur J Nucl Med Mol Imaging 37:517–521
23. Mylonas I, Kazmi M, Fuller L, deKemp RA, Yam Y, Chen L et al (2012) Measuring coronary artery calcification using positron emission tomography-computed tomography attenuation correction images. Eur Heart J Cardiovasc Imaging 13:786–792
24. Cerqueira MD, Weissman NJ, Dilsizian V, Jacobs AK, Kaul S, Laskey WK et al (2002) Standardized myocardial segmentation and nomenclature for tomographic imaging of the heart: a statement for healthcare professionals from the Cardiac Imaging Committee of the Council on Clinical Cardiology of the American Heart Association. J Nucl Cardiol 9:240–245
25. Slomka PJ, Alexanderson E, Jacome R, Jimenez M, Romero E, Meave A et al (2012) Comparison of clinical tools for measurements of regional stress and rest myocardial blood flow assessed with 13N-ammonia PET/CT. J Nucl Med 53:171–181
26. Hutchins GD, Schwaiger M, Rosenspire KC, Krivokapich J, Schelbert H, Kuhl DE (1990) Noninvasive quantification of regional blood flow in the human heart using N-13 ammonia and dynamic positron emission tomographic imaging. J Am Coll Cardiol 15:1032–1042
27. Sadeghi M, Schwartz R, Beanlands R, Al-Mallah M, Bengel M, Borges-Neto S et al (2011) Cardiovascular nuclear imaging: balancing proven clinical value and potential radiation risk. J Nucl Med 52:1162–1164
28. ICRP publication 80 (1998) Radiation dose to patients from radiopharmaceuticals. Pergamon Press, Oxford